

Supplement of Atmos. Chem. Phys. Discuss., 15, 2997–3061, 2015
<http://www.atmos-chem-phys-discuss.net/15/2997/2015/>
doi:10.5194/acpd-15-2997-2015-supplement
© Author(s) 2015. CC Attribution 3.0 License.



Supplement of

Nighttime measurements of HO_x during the RONOCO project and analysis of the sources of HO₂

H. M. Walker et al.

Correspondence to: D. E. Heard (d.e.heard@leeds.ac.uk)

1 Supplementary Information

3 1 Leeds Aircraft FAGE instrument characterisation

4 1.1 Instrument calibration

5 The results from the February 2011 calibration, following the winter RONOCO fieldwork,
6 are shown in Fig. S1.

7 1.2 Factors affecting sensitivity

8 The theoretical sensitivity, as a function of the detection cell pressure, is given by:

$$9 \quad C(P_{\text{cell}}) = D \cdot T_{\text{OH}} \cdot \phi_f \cdot f_{\text{gate}} \cdot [\text{OH}]_{\text{cell}} \quad (1)$$

10 where P_{cell} is the pressure inside the detection cell, D is a collective term for pressure-
11 independent variables (laser power, OH absorption cross-section, laser linewidth, physical
12 overlap of laser and gas beams, solid angle of fluorescence collection, transmission of
13 collection optics, quantum yield of the channel photomultiplier tube), T_{OH} is the transmission
14 of OH through the inlet and pre-detection assembly, ϕ_f is the OH fluorescence quantum
15 yield, f_{gate} is the fraction of the total OH fluorescence detected within the photon counter
16 gate, and $[\text{OH}]_{\text{cell}}$ is the number density of OH in the detection cell (Creasey et al., 1997;
17 Faloon et al., 2004; Heard, 2006; Dusanter et al., 2009). Apart from the laser power, the
18 terms contributing to D remain constant throughout a measurement period, and are accounted
19 for by regular calibrations. Laser power is measured by photodiodes positioned in the OH and
20 HO₂ detection cells, and the recorded OH and HO₂ signals are normalised to the measured
21 laser power.

22 1.2.1 Effects of water vapour concentration on sensitivity

23 The fluorescence quantum yield, ϕ_f , is given by the ratio of the rate of radiative decay to the
24 total rate of decay:

$$25 \quad \phi_f = \frac{\tau^{-1}}{\Gamma} = \frac{k_{\text{rad}}}{k_{\text{rad}} + \sum_i k_{\text{qi}} [q_i]} \quad (2)$$

26 where τ is the fluorescence lifetime of the OH in the absence of quenchers (= 688 ns)
 27 (German, 1975), Γ is the total rate of decay of excited OH, $k_{\text{rad}} = \frac{1}{\tau_{\text{rad}}}$ is the rate constant
 28 for radiative decay, k_{q_i} is the rate constant for quenching of the OH fluorescence by ambient
 29 molecule i , and $[q_i]$ is the number density of the quenching species i . N_2 , O_2 , and H_2O are the
 30 most important atmospheric quenchers of OH fluorescence. The ambient mixing ratios of N_2
 31 and O_2 are constant. The ambient concentration of water vapour, however, varies sufficiently
 32 (0–4 %) that its effect on instrument sensitivity must be taken into account during field
 33 measurements (Stevens et al., 1994). The fraction of OH fluorescence collected within the
 34 photon counting gate, f_{gate} , is dependent on the OH fluorescence lifetime, and therefore on the
 35 rate of quenching by water vapour.

36 Given a measured sensitivity at a known water vapour concentration, the theoretical
 37 reduction or increase in sensitivity at other water vapour concentrations can be calculated.
 38 The fraction of OH fluorescence collected in the photon counting gate, f_{gate} , and the
 39 fluorescence quantum yield, ϕ_f , are given by:

$$40 \quad f_{\text{gate}} = e^{-\Gamma t_1} - e^{-\Gamma t_2} \quad (3)$$

$$41 \quad \phi_f = \frac{\tau^{-1}}{k_{\text{rad}} + k_{q,\text{N}_2} [\text{N}_2]_{\text{cell}} + k_{q,\text{O}_2} [\text{O}_2]_{\text{cell}} + k_{q,\text{H}_2\text{O}} [\text{H}_2\text{O}]_{\text{cell}}} \quad (4)$$

42 where $t_1 = 110$ ns and $t_2 = 1110$ ns are the start and end times of the photon-counting gate,
 43 respectively, and $[\text{N}_2]_{\text{cell}}$, $[\text{O}_2]_{\text{cell}}$, and $[\text{H}_2\text{O}]_{\text{cell}}$ are the concentrations inside the detection
 44 cell. Knowledge of the ambient pressure and the detection cell pressure enables calculation of
 45 $[\text{N}_2]_{\text{cell}}$, $[\text{O}_2]_{\text{cell}}$, and $[\text{H}_2\text{O}]_{\text{cell}}$, and therefore f_{gate} and ϕ_f , for any ambient water vapour
 46 concentration which was measured on the aircraft. Since C_{OH} is directly proportional to the
 47 product of f_{gate} and ϕ_f , a correction factor can be applied to C_{OH} as follows:

$$48 \quad C_{\text{OH}}(\text{H}_2\text{O}) = C_{\text{OH,meas}} \cdot \frac{f_{\text{gate}} \cdot \phi_f}{f'_{\text{gate}} \cdot \phi'_f} \quad (5)$$

49 where f_{gate} and ϕ_f are the values calculated for a calibration at a known water vapour
 50 concentration, and f'_{gate} and ϕ'_f are the values calculated for other water vapour
 51 concentrations.

52 A summary of ambient and detection cell water vapour concentrations and the instrument
53 sensitivity to OH and HO₂ during the RONOCO and SeptEx field measurement campaigns is
54 given in Table S1. The range of ambient water vapour concentrations exceeds the range that
55 can be reliably achieved during a calibration. For this reason, theoretical water-dependent
56 sensitivities were calculated for the RONOCO and SeptEx data, using the ambient water
57 vapour concentration, the ambient pressure, and the detection cell pressure measured during
58 the flights, to adjust the sensitivities measured during the calibrations that followed each
59 measurement campaign.

60 1.2.2 Effects of pressure on sensitivity

61 The pressure inside the detection cell, P_{cell} , changes with external pressure during aircraft
62 FAGE measurements. The internal pressure affects a number of parameters in Eq. (6),
63 namely the number density of OH inside the detection cell, $[\text{OH}]_{\text{cell}}$, OH transmission, T , OH
64 fluorescence quantum yield, ϕ_f , and therefore the fraction of OH fluorescence detected in the
65 photon counting gate, f_{gate} .

66 The experimental pressure dependence of C_{OH} and C_{HO_2} has been investigated by Commane
67 (2009; see also Commane et al., 2010) following the method of Faloon *et al.* (2004) and
68 Martinez *et al.* (2010). The pressure inside the detection cell can be varied between 1.6 and
69 2.7 Torr by varying the diameter of the inlet pinhole between 0.50 and 0.85 mm, to mimic a
70 change in external pressure. Calibrations can therefore be conducted over a range of cell
71 pressures applicable to aircraft-based measurements. During the RONOCO aircraft
72 campaign, P_{cell} ranged between a maximum of 1.9 Torr at ground level to 1.2 Torr at 6 km.
73 C_{OH} and C_{HO_2} were found to be independent of pressure over the range of pressures
74 experienced during typical aircraft-based measurements, and within the reproducibility of
75 calibration results, in agreement with the theoretical calculations.

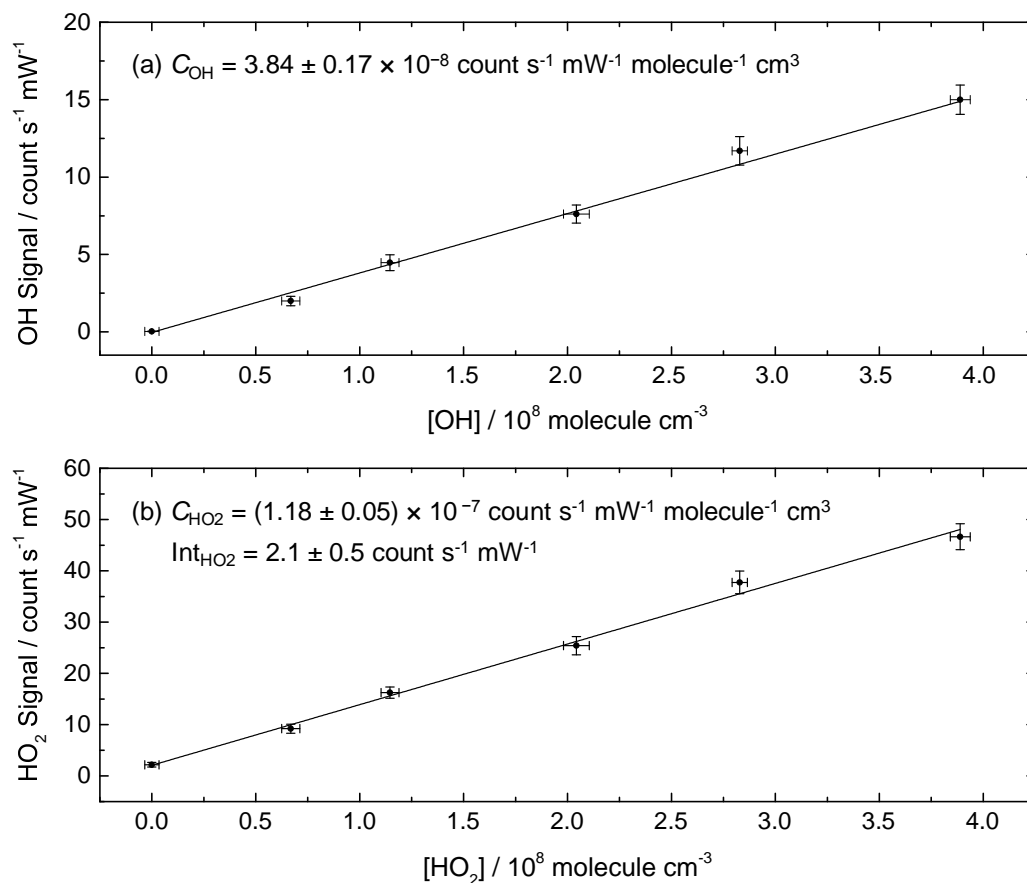
76 The pressure-dependent calibration method using different sized pinholes relies on the
77 assumptions that losses of OH and HO₂ to the inside of the pinhole does not change
78 significantly with pinhole diameter, and that the flow regime remains similar for pinholes of
79 different diameter. The method has been validated by calibration of the aircraft FAGE
80 instrument for sensitivity to HO₂ at different external pressures inside the atmospheric
81 simulation chamber HIRAC at the University of Leeds using the photolysis of formaldehyde
82 followed by time-dependent measurements of HO₂ (Winiberg et al., 2014). The FAGE inlet
83 was positioned inside the chamber, with the detection cells located outside the chamber. The

84 pressure inside the detection cells ranged between 1.1 and 1.9 Torr. Little variation in C_{HO_2}
85 was found over the range of pressures studied, in agreement with the results of Commane
86 (2009). At 1.1 Torr, C_{HO_2} was $8.0 \pm 1.6 \times 10^{-8}$ count s^{-1} mW^{-1} molecule $^{-1}$ cm^3 , and at
87 1.9 Torr C_{HO_2} was $1.2 \pm 0.24 \times 10^{-7}$ count s^{-1} mW^{-1} molecule $^{-1}$ cm^3 , the two values being the
88 same within their combined uncertainties.

89 Table S1. Ambient and detection cell water vapour concentrations, C_{OH} , and C_{HO2} during
 90 RONOCO and SeptEx. Mean values are given in parentheses.

	RONOCO summer, 2010	SeptEx, 2010	RONOCO winter, 2011
Ambient $[H_2O] / 10^{17}$ molecule cm^{-3}	1.03–3.55 (2.64)	0.318–3.63 (2.34)	0.016–4.37 (1.49)
Detection cell $[H_2O] /$ 10^{14} molecule cm^{-3}	2.64–9.18 (6.67)	0.648–8.86 (5.60)	0.004–10.6 (3.43)
$C_{OH} / \text{count s}^{-1} \text{ mW}^{-1}$ molecule $^{-1} \text{ cm}^3$	3.0×10^{-8}	3.0×10^{-8}	3.8×10^{-8}
C_{OH} corrected for mean $[H_2O] / \text{count s}^{-1} \text{ mW}^{-1}$ molecule $^{-1} \text{ cm}^3$	2.9×10^{-8}	3.1×10^{-8}	4.3×10^{-8}
$C_{HO2} / \text{count s}^{-1} \text{ mW}^{-1}$ molecule $^{-1} \text{ cm}^3$	9.3×10^{-8}	9.3×10^{-8}	1.1×10^{-7}
C_{HO2} corrected for mean $[H_2O] / \text{count s}^{-1} \text{ mW}^{-1}$ molecule $^{-1} \text{ cm}^3$	9.5×10^{-8}	9.6×10^{-8}	1.2×10^{-7}

91



92

93 Figure S1. Results from a calibration of the aircraft FAGE instrument in February 2011,
 94 following the winter RONOCO fieldwork, at $[\text{H}_2\text{O}] = 9 \times 10^{16} \text{ molecule cm}^{-3}$ (0.4 %). Data
 95 points represent average values for one minute of online data. x and y error bars represent the
 96 standard deviations of $[\text{OH}]$ and $[\text{HO}_2]$, and the normalised FAGE signals, respectively. The
 97 instrument sensitivity to OH, C_{OH} , is equal to $(3.84 \pm 0.17) \times 10^{-8} \text{ count s}^{-1} \text{ mW}^{-1}$
 98 $\text{molecule}^{-1} \text{ cm}^{-3}$. The instrument sensitivity to HO₂, C_{HO_2} , is equal to $(1.18 \pm 0.05) \times 10^{-7}$
 99 $\text{count s}^{-1} \text{ mW}^{-1} \text{ molecule}^{-1} \text{ cm}^{-3}$. The intercept of the HO₂ calibration plot, an artefact caused
 100 by the addition of NO, is equal to $2.1 \pm 0.5 \text{ count s}^{-1} \text{ mW}^{-1} \text{ molecule cm}^{-3}$.